*Science of Sintering*, **53** (2021) 155-167

https://doi.org/10.2298/SOS2102155D

UDK: 53.086; 546.74; 692.533.1; 676.017.5

# Incandescent Combustion Synthesis of Nanomagnetic Ni/NiO Composites

**Nasrallah M. Deraz**[*)]
Physical Chemistry Department, National Research Centre, 33 El Bohouth St., Dokki, Giza, P.O.12622, Egypt

***Abstract:***

*This study is the first attempt to large-scale energy-efficient production of nanomagnetic Ni/NiO composites by using the autocombustion based on leaves or extract of corchorus olitorius. The as synthesized product can be characterized by using XRD, SEM, TEM and EDX techniques. The results confirm that the as synthesized materials consisted entirely of well crystalline Ni and NiO phases. The crystallinity of both Ni and NiO enhanced by increasing amount of the corchorus olitorius. However, the corchorus olitorius - treatment resulted in an increase in the crystallite size and lattice constant. The SEM analysis confirms formation of fragile, fluffy and spongy networks. The average of grain size for the as prepared particles was found to be 45 nm in agreement with the trend of the crystallite size calculated by using XRD technique. Furthermore, changing of nature and content of the corchorus olitorius brought about progressive modifications in the magnetic properties, namely, Ms, Mr, Mr/Ms, Hc and Ka, of the fabricated Ni/NiO nanocomposite according to the structural, morphological as well as microstructural variation. The saturation magnetization (Ms) of the sample with corchorus olitorius leaves was found to be 0.2383 emu/g while the Ms with corchorus olitorius extract was found to 6.977 emu/g. This was discussed in the light of finite size, surface and interface effects. Thus, we unveil a new approach for incandescent combustion synthesis via an innate approach for corchorus olitorius leaves in the directly fabrication for different nanocomposites.*

***Keywords****: XRD; SEM; SBET; Corchorus olitorius leaves; Magnetic properties.*

## 1. Introduction

Magnetic systems containing two or more components exhibit novel and unique properties due to the interactions between the constituents. Properties of any system composed of multi-component particles depend on their size, structure and composition. In fact, the multi-component system has more extensive applications than a single-component system [1-4]. Nickel-based nano materials have gained considerable attention due to their applications in various fields such as catalysis, fuel cell electrodes, gas sensors, supercapacitors, smart windows, data storage and spintronic devices [5, 6]. Ferromagnetic (FM) metal such as nickel (Ni) and antiferromagnetic (AFM) metal oxide such as nickel oxide (NiO) subjected to growing interest due to their interesting properties and wide range of applications [7-9].

Bi-magnetic nanoparticles demonstrate different effects such as tunable blocking temperatures, large exchange bias tailored coercivities, high resonance fields or proximity

[*)] **Corresponding author:** nmderaz@yahoo.com

effects and two-stage magnetization reversal [10]. On other hand, combination of the FM and AFM materials can be fabricated in various forms such as core – shell, layered film, nano granular and nanocomposites. [11]. Ni/NiO nanocomposites exhibit interesting applications in diverse fields such as lithium ion batteries, electro catalysts for hydrogen evolution reaction and electrochemical energy storage [12]. These applications depend upon the unique properties of these composites such as thermal stability and magnetic properties [13]. However, these properties have a direct correlation with the grain size, morphology and the crystalline phases in the Ni/ NiO nanocomposites [14].

In fact, the preparation routes of Ni/NiO nano particles influence on the purity, crystallinity, metal oxidation state, stoichiometry of final product. In addition, these particles nanoparticles were prepared by using different methods such as chemical precipitation, sol–gel method, hydrothermal growth, solvothermal process, microemulsion method, solid-state chemical decomposition, ball milling, organometallic route, and magnetron plasma [15-21]. Unfortunately, these techniques need long reaction times with consuming high-energy. Recently, when considering ideally techniques to synthesize perovskite and spinel based materials; they should require minimal steps and mild conditions [25, 26]. It was demonstrated that the presence of reducing agent during preparation of the perovskite and spinel systems lowers energy consumption in the preparation process [27].

Nowadays, the auto combustion route is popular method for formation of porous metal and metal oxide particles because of simplicity, rapidly, cost effective and low temperature requirement [25, 26]. Our previous works reported to prepare of Ni/NiO system via the combustion method by using glycine as fuel [26]. Our previous results confirmed formation of nanocrystalline Ni/NiO composites. In addition, Ni was formed as a single phase when the molar ratio of glycine to nitrate was 1.5.

Furthermore, there is an increasing tendency to develop combustion method for the synthesis of different nano materials by using various parts of plants such as leaves, stems, roots, shoots, flowers, barks and seeds [27]. The extracts of these parts play role of fuels in combustion route to prepare of various greener nanoparticles such as silver, gold and magnetite [28]. These fuels act as reducing and stabilizing agents for the bio reduction reaction in the synthesis of various metallic nano particles by combustion process [29].

In this study, we display a novel method for synthesis and easy control of the size and composition of Ni/NiO composite particles via combustion method by using dried leaves of corchorus olitorius and its extract.

## 2. Materials and Experimental Procedures

### 2.1. Chemicals and Plant Material Collection

The chemical material was copper (II) nitrate trihydrate with linear formula $Ni(NO_3)_2 \cdot 6H_2O$ and supplied by Sigma-Aldrich Company. This reagent was of analytical grade and used without further purification. Fresh corchorus olitorius leaves were collected from a local field.

### 2.2. Preparation route

#### *2.2.1. Preparation of leaf extracts and leaf powder*

Firstly, fresh corchorus olitorius leaves were collected and washed with tap water with subsequent washing again with distilled water until no impurities remained. Then, the fresh leaves were cut into small pieces and left it in the air for a week to dry completely. Dry leaves were crushed well to use as a leaf powder or to make the leaf extract. 1.5 g was weighed and put into a beaker with 20 ml of distilled water. The mixture was heated for 30

minutes at 70 °C with vigorous stirring without pH adjustment and then allowed to cool at room temperature. Then, the mixture was filtered yielding the extract which stored in the refrigerator for further use to synthesize Ni/NiO nanocomposite from nickel nitrate precursor solution.

### *2.2.2. Preparation of Ni/NiO nanocomposites*

Three samples were prepared by mixing the obtained extract or 0.5 g or 1.5 g from the dried leaves of corchorus olitorius with 2.91 g of nickel nitrate precursor solution. The mixed solutions were concentrated in a Pyrex beaker (100 ml) on a hot plate at 350 °C for quarter hour. The crystal water was gradually vaporized during heating and when a beaker temperature was reached to 350 °C, a great deal of foams produced and spark appeared at one corner which spread through the mass with incandescent combustion, yielding a voluminous and fluffy product in the container. The prepared solid samples were designated as S1, S2 and S3 for nickel nitrates which treated with 20 ml leaf extract, 0.5 g and 1.5 g from leaves of corchorus olitorius, respectively.

## 2.3. Techniques

An X-ray measurement of various mixed solids was carried out using a BRUKER D8 advance diffractometer (Germany). The patterns were run with Cu $K_\alpha$ radiation at 40 kV and 40 mA with scanning speed in 2θ of 2° $min^{-1}$.

The crystallite sizes of crystalline phases present in the investigated solids was based on X-ray diffraction line broadening calculated by using Scherrer equation [30].

$$d = \frac{B\lambda}{\beta \cos\theta} \quad (1)$$

where d is the average crystallite size of the phase under investigation, $B$ is the Scherrer constant (0.89), $\lambda$ is the wave length of X-ray beam used, $\beta$ is the full-width half maximum (FWHM) of diffraction and $\theta$ is the Bragg's angle.

The JEOL JAX-840A scanning electron micro-analyzer (SEM) and JEOL Model 1230 (Jeol, Tokyo, Japan) transmittance electron micro-analyzer (TEM) have captured scanning and transmittance electron micrographs of the as prepared solid, respectively. The solid as it had been handled was washed in ethanol, and then ultrasonically adjusted to disperse individual particles over a small piece double stick Carbon tape putted over mount holders.

Energy dispersive X-ray analysis (EDX) was carried out on JEOL (JED- 2200 Series) electron microscope with an attached kevex Delta system. The parameters were as follows: accelerating voltage 15 kV, accumulation time 100 s, window width 8 $\mu$m. The surface molar composition was determined by the Asa method, Zaf-correction, Gaussian approximation.

The surface characteristics of various solid catalysts, namely, the specific surface area ($S_{BET}$), total pore volume ($V_p$) and mean pore radius (r̄) were determined from nitrogen adsorption isotherms measured at 77 K, using Nova 2000, Quanta Chrome (commercial BET unit). Before undertaking such measurements, each sample was degassed under a reduced pressure of 0.00133 Pa for 2 h at 200 °C.

The magnetic properties of the investigated solid were measured at room temperature using a vibrating sample magnetometer (VSM; 9600-1 LDJ, USA) in a maximum applied field of 20 kOe. From the obtained hysteresis loops, the saturation magnetization ($M_s$), remanence magnetization ($M_r$), the squerence ($M_r/M_s$) and coercivity ($H_c$) were determined.

## 3. Results and Discussion

### 3.1. Structural analysis

XRD analysis confirms formation Ni/NiO nanocomposite by using corchorus olitorius leaves assisted combustion method at low temperature (350 °C) for few minutes. Fig. 1 displays XRD patterns for the S1, S2 and S3 samples. The XRD pattern revealed that the nickel powders (Ni and NiO) crystallize with a cubic structure and the space group *Fm3m*, which are well matched with the reported values in JCPDS files (No. 04-0850 and No. 04.0835, respectively. Indeed, the main peaks of NiO are observed at angles for 2θ = 37.47°, 43.46°, 62.98° and 79.10°, in addition, these peaks correspond to (*hkl*) planes (111), (200), (220) and (311), respectively. While, the main peaks of Ni are detected at angles for 2θ = 44.76°, 51.75° and 79.10°, however, these peaks correspond to (*hkl*) planes (111), (200) and (220), respectively. One cannot ignore presence of traces of carbon as a combustion product which is not observed in XRD pattern due to its small quantity.

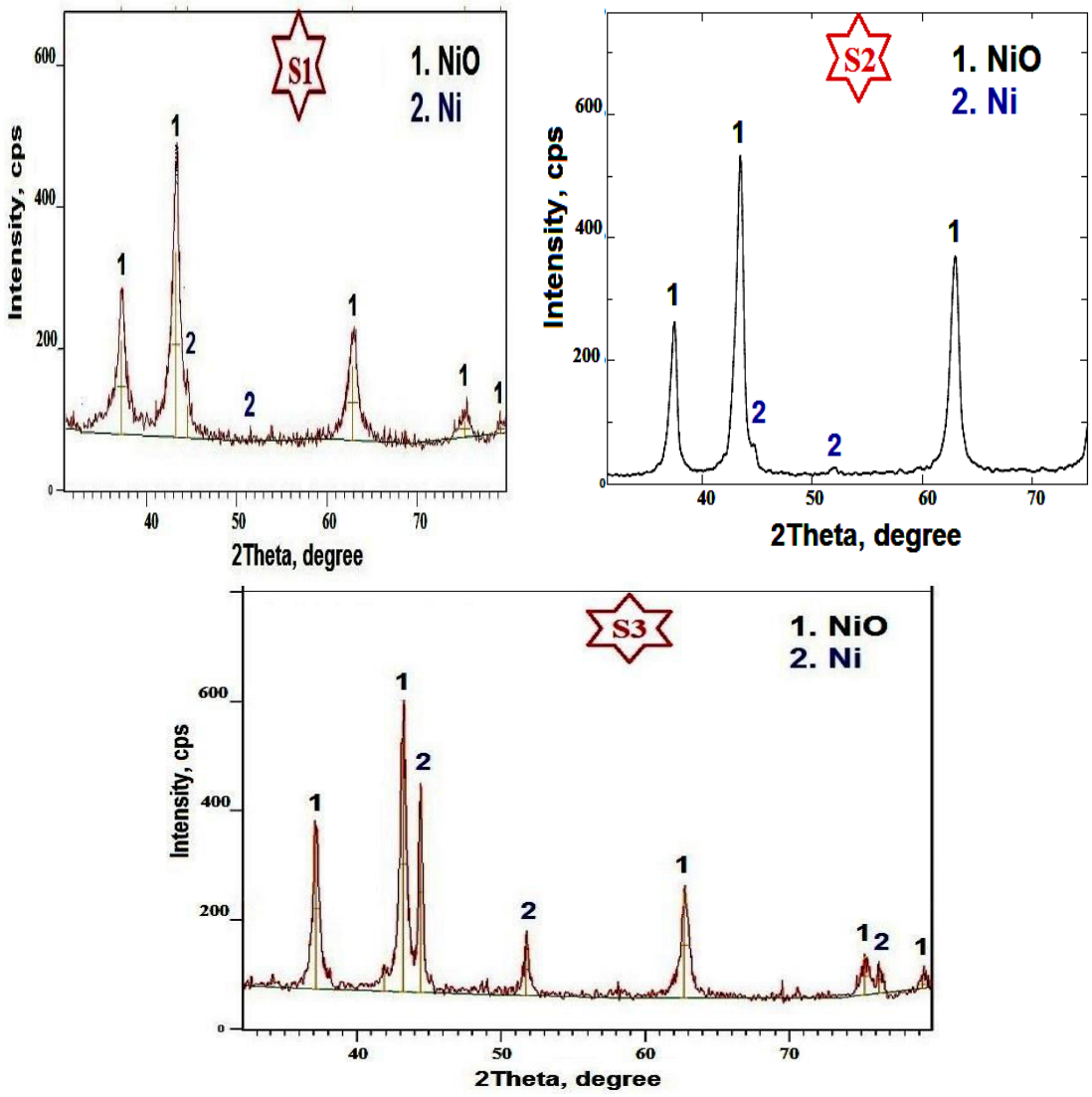


**Fig. 1.** XRD patterns of the as prepared system: (a) S1, (b) S2 and (c) S3.

XRD patterns showed that the abundance of both Ni and NiO depends upon the amount and nature of corchorus olitorius leaves. The extract of 1.5 g of corchorus olitorius leaves resulted in appearance small amount of Ni which increased by directly mixing of the dry leaves with the nickel precursor. The same behavior was observed by increasing the dried leaves of corchorus olitorius content from 0.5 g to 1.5 g. In fact, the percentages of Ni in the S1, S2 and S3 samples are found to 10, 25 and 45 %, respectively.

There will be no exaggeration when we say that this is the first time that a Ni/NiO nanocomposite has been prepared by using dry corchorus olitorius leaves. In addition, the high percentage (45 %) for formation of metallic nickel nanoparticles was not expected. Indeed, this leaves stimulate the reduction of the metallic salt, yielding high amount of Ni nanoparticles. This can prevent Ni oxidation and also simplifies the process and paves the way for formation of Ni.

The mechanism of dry corchorus olitorius leaves assisted combustion method, followed by the formation of metallic nickel, can be discussed as following: (i) a strong exothermic reaction resulted in an increase of the temperature favoring a fast thermal decomposition of the precursors. (ii) Reduction of metallic salt (nickel nitrate) can be achieved by bioreductant agents based biomolecules. Indeed, the plant and plant parts contain abundant biomolecules (natural compounds) such as alkaloids, flavonoids, sapo nins, steroids, tannins, and other nutritional compounds [31]. (ii) Stabilization and prevention of oxidation of Ni nanoparticles is done through carbon, which is a protective agent of Ni. In fact, a fast decomposition of the precursors brought about formation of Ni/NiO nanocomposite with subsequent carbon formation. Similar studies were observed with different systems [31-35]. Results of these studies have been suggested Ni formation as a result of both the decomposition of the precursors and the protection of Ni by graphite. The deep involvement of dry corchorus olitorius leaves in the combustion procedure by increasing amounts may favor a more reductive atmosphere with subsequent increase in the Ni content.

X-ray results enable us to study the effect of fuel on some structural parameters such as the crystallite size (d), lattice constant (a) and unit cell volume (V) of crystalline phases. The calculated values of different structural parameters are given in Table I. As shown in this table that the "a, V and d " values of NiO are greater than that of Ni. This will allow NiO particles to be covered in a lot of metallic Ni particles.

**Tab. I** Lattice parameters of Ni and NiO phases.

| Parameters / Sample | Ni | | | NiO | | |
|---|---|---|---|---|---|---|
| | d, nm | a, nm | V, $nm^3$ | d, nm | a, nm | V, $nm^3$ |
| S1 | 17 | 3.5042 | 43.029 | 23 | 4.1610 | 72.043 |
| S2 | 15 | 3.5132 | 43.362 | 20 | 4.1711 | 72.569 |
| S3 | 24 | 3.5310 | 44.024 | 29 | 4.1869 | 73.397 |

From this table, the maximum increase in the values of a, V and d values of Ni and NiO was observed in case of the S3 sample. The observed increase in the values of a, d and V for Ni and NiO solids could be attributed to an increase in the flame temperature which stimulate crystal growth and/or particles adhesion. In spite of that the crystallite sizes of the as prepared samples are too small and less than 100 nm. Similar observations were reported on different metal oxide systems with various discussions depend on the strong repulsive interactions of parallel surface defect dipole, the valence reduction and unpaired electron orbital at outer surface [36-38].

### 3.2. Surface morphology

The surface morphology of the S3 sample was determined to obtain information about the morphological properties of Ni/NiO composite. Fig. 2 a-c displays SEM images for the S3 sample with different magnifications. These images show fragile sponge islands which consisted entirely of crystalline particles.

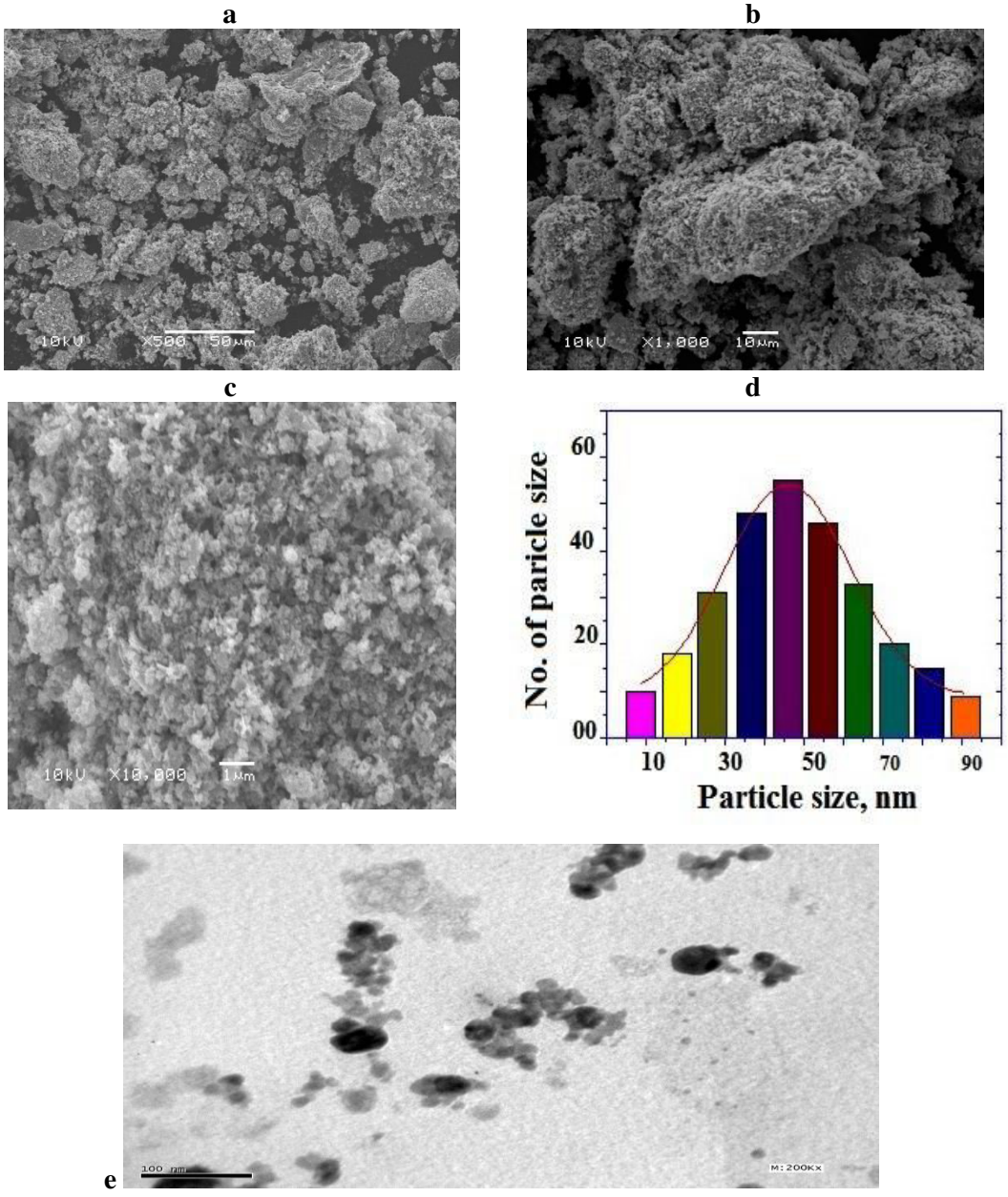


**Fig. 2.** The histogram of size and SEM images with different magnifications for the S3 sample; (a) 500x, (b) 1000x, (c) 10000x magnification, (d) histogram of size and (e)TEM image.

Checking the shape of these particles indicated they have spherical, ellipsoidal and irregular morphologies. Voids and pores can be found on the prepared solid surface due to libration of gas molecules during the decomposition of the nickel–fuel precursors. The average particle

size of the S3 sample was 45 nm as shown in the histogram for particle size distribution, Fig. 2e, which illustrated based on SEM micrograph [39]. However, we can be seen bright areas correspond to the Ni particles and faint grey areas related to NiO particles which shows less heavy scatters. In addition, there is a lower contrast darker porous material which is a carbonaceous by-product. In other words, we can be speculated that the porous material (a carbonaceous by-product with low contrast light) is mixed with variable contrast light Ni/NiO nanoparticles. This finding shows that the majority of sample consists of small NiO and carbon particles with large Ni areas. These areas brought about formation of the Ni/NiO interfaces with subsequent appearance of the exchange bias field. Thus, we can be guess that the combustion process favors the formation of NiO on uppermost surface of the Ni particles with some impurities from carbon. In addition, NiO and carbon particles act as isolating regions to prevent the further growing of Ni nano particles with a disordered growth of the NiO matrix [40, 41].

The dry corchorus olitorius leaves assisted combustion method for green synthesis of Ni/NiO nanocomposite was completed at 350 $^{o}$C within a few minutes. In fact, the conventional solution combustion synthesis for different materials usually emerges explosive behavior. In this study, the current combustion is relatively slower and more moderate in a self-propagating mode with lithe and relatively high product. Herein, we observed the presence of heat-resistant dry corchorus olitorius leaves in a new type of self-organization in combustion via the incandescent liquid spheroidal formation [42]. The product often is fluffy, fragile and spongy yielding porous material with unique properties.

An additional TEM analysis, about the crystal nature of Ni and NiO NPs, was carried out on the S3 sample as shown in Fig. 2e. This figure confirms that the synthesized material had homogenous structures and sizes ranged in the nanometer scale. Ni/NiO NPs tend to be smaller in sizes and sporadically dispersed with some agglomerations. EDX analysis can be used to determine the elemental composition of the investigated samples. Fig. 3 displays the EDX pattern of the S3 sample as representative specimen for all samples. According to EDX pattern, the S3 sample is composed by higher weight percentage of nickel and trace amount of carbon and oxygen. The characteristic signals of the elements of nickel (Ni), oxygen (O), and carbon (C) were calculated in Fig. 3. Ni: 64.85 wt percent, O: 24.23 wt percent and C: 10.92 wt percent, respectively, were the weights percent of nickel, oxygen and carbon measured from EDS. However, the quantity of oxygen is low indicating the formation of comparatively larger amount of Ni. These results confirm that our preparation method is more promising one for obtaining of Ni/NiO NPs with minimal particle size and free carbon content.

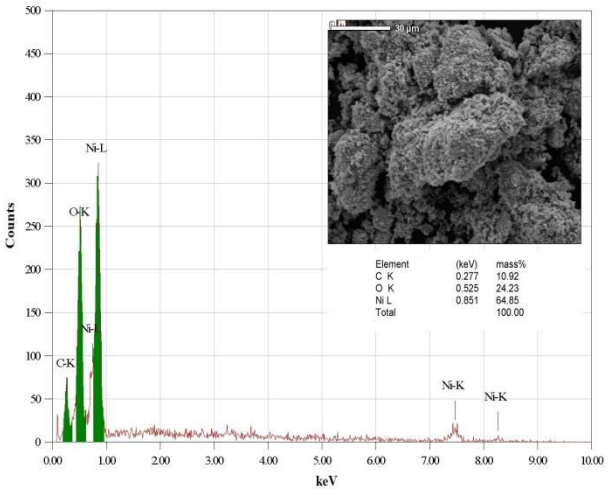


**Fig. 3.** EDX pattern of the S3 sample.

### 3.3. Surface properties

Various surface properties, namely $S_{BET}$, $V_p$, and r̂ for the as synthesized composites were investigated from $N_2$ adsorption isotherms conducted at 77 K. The obtained results are given in Table II. This table confirms that the $S_{BET}$ of the S3 sample greater than that of the S1 sample. This difference could be attributed to a pore-narrowing process depending upon a decrease of the r̂ value of the S3 sample. The maximum decrease in mean pore radius was found to be 21.8 %, while the maximum increase in the surface area was 117.5 % for the S3 sample. In other words, the porosity of Ni/NiO nanocomposite increases as the corchorus olitorius leaves content increases depending upon an increase in the total pore volume of sample. It is expected that an increase in the surface area and total pore volume will lead to an increase in size and interface effects with subsequent increase in both the coercivity and magnetization of composites.

**Tab. II** Surface properties of the as prepared samples.

| Samples | $S_{BET}$ ($m^2/g$) | $V_p$ ($cm^3/g$) | r̂ (nm) |
|---|---|---|---|
| S1 | 7.34 | 0.0021 | 11.66 |
| S2 | 9.43 | 0.0120 | 10.42 |
| S3 | 15.97 | 0.0822 | 9.11 |

### 3.4. Magnetic properties

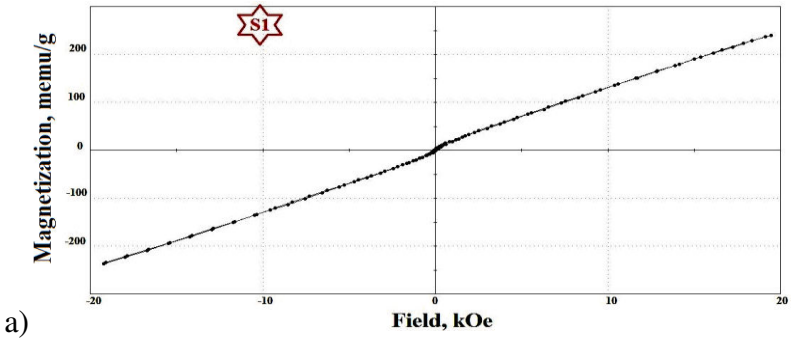


a)

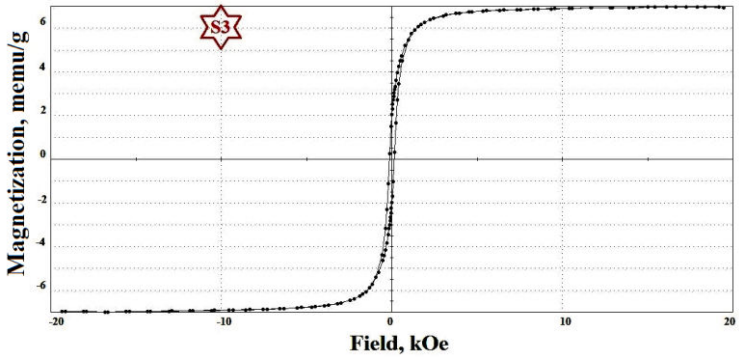


b)

**Fig. 4.** *M-H* curve for the as synthesized samples; (a) S1 and (b) S3 samples.

The effect of fuel content dependent nanocrystalline microstructure on the magnetic properties was determined for the S1 and S3 samples by a vibrating sample magnetometer, at room temperature with an applied magnetic field between -20kOe to +20kOe. The magnetization versus magnetic field plots (measurements of M–H magnetic hysteresis loops) for the S1 and S3 samples are shown in Fig. 4a and b. However, the magnetic characteristics for such samples are listed in Table III. The S1 samples exhibited vanished hysteresis as shown in Fig. 4a. In all field regions, the increase of magnetization for the S1 sample slows down as the applied magnetic field increases. For the S3 sample, the magnetization increases significantly with increasing applied field in lower-field region. However this increase slows down as we further increase the applied magnetic field as shown in Fig. 4b. These observations resulted to construction of the hysteresis loops confirming the different natures of the S1 and S3 samples at room temperature [43]. As seen from Table III that values of $M_s$, $M_r$, $M_r/M_s$, $H_c$ and $K_a$ for the S3 sample are greater than that for the S1 sample.

**Tab. III** The magnetic properties ($M_s$, $M_r$, $M_r/M_s$, $K_a$ and $H_c$) for the S1 and S3 samples.

| **Samples** | **$M_s$ (emu/g)** | **$M_r$ (emu/g)** | **$M_r/M_s$ (emu/g)** | **$H_c$ (Oe)** | **Anisotropy constant ($K_a$)** |
|---|---|---|---|---|---|
| S1 | 0.2383 | $1.935 \times 10^{-3}$ | $5.945 \times 10^{-3}$ | 61.87 | 15.04 |
| S3 | 6.977 | 1.956 | 0.283 | 135.77 | 966.6 |

Indeed, NiO is one bulk antiferromagnets which does not show net manetization. On the other hand, NiO nanoparticles or the nanoscale antiferromagnet may possess magnetization due to the minimization of thermal vibration energy and the surface uncompensated spins. However, the nanosized NiO powders have non-stoichiometric nature which correlated to the development of surface disorder via formation of $Ni^{3+}$ ion in the NiO lattice yielding the paramagnetism at room temperature [44]. In this case, the exchange interaction between two neighbouring $Ni^{2+}$ ions is mediated by an oxygen ion through superexchange interaction [45]. Thus, fine particles of antiferromagnetic (AFM) nature should exhibit either a weak ferromagnetism (FM) or superparamagnetism (SPM). This confirms the size dependent magnetic characteristics of NiO.

The coexistence of Ni and NiO in the as prepared samples resulted in appearance of the exchange bias (EB) effect which originates at the interface between two magnetically different phases, typically a ferromagnet (FM) and an antiferromagnet (AFM). The EB effect critically depends on the microstructure of the interface (roughness and crystallinity degree) that determines the spin configuration [46]. The EB effect and the anisotropy energy for the Ni-rich sample are larger than the interface exchange interaction energy and vice versa for NiO-rich sample. Table III shows the change of magnetization for the resulted composites according to the amount and nature of the corchorus olitorius leaves. It can see from this table that both the magnetization and coercivity for the S3 sample are greater than that of the S1 sample.

Indeed, the increase in values of coercivity for the S3 sample is probably due to an increase in magnetocrystalline anisotropy [47]. In contrast, the decreasing trend of anisotropic constant ($K_a$) value resulted in a decrease in magnetostatic energy for the S1 sample. However, the lattice expansion in the presence of defects and surface anisotropy plays a significant role in controlling the interaction between the uncompensated surface spins and bulk particle spins. These results display that the resulting magnetic properties of the as synthesized composite are very complex due to the interplay between finite size, surface effects and interface effects. Finally, the $M_s$ of Ni/NiO composite in this study compared with that reported for this

composite in our previous study exhibited a large difference due to weak magnetic interfaces which contains nonmagnetic residual carbon and antiferromagnetic nickel oxide layer covered on the surface of metallic Ni nanoparticles [26].

## 4. Conclusion

Fabrication of Ni/NiO nano particles based composites is accomplished by using a facile combustion route. Magnetic behavior of the as synthesized composites corresponding to the nanoscale size effect was observed. XRD measurements showed an order changes in the structural properties of the as prepared composites. These changes can be ascribed to the transition between metallic nickel and nickel oxide. The amount and nature of corchorus olitorius leaves affect in the abundance of both Ni and NiO. However, XRD results confirm formation of Ni/NiO nanocomposites with different crystallite sizes for Ni NiO phases. The change of both amount and nature of the corchorus olitorius leaves brought about different modifications in the porosity of the as prepared nanocomposites. In addition, the magnetic properties of a nanocomposite based device can be tuned in the desired range by suitably modifying Ni/NiO transition. However, the magnetization of the composite prepared by using the dry corchorus olitorius leaves assisted combustion was excellent compared to the magnetization of the composite synthesized by using the extract of the same amount from the corchorus olitorius leaves. Finally, we speculate that this straightforward approach can further be extended to synthesize other metal/metal oxide nanocomposites for electrical, magnetic and allied applications.

## 5. References

1. Devan, R. S.; Ranjit A. Patil, R. A.; Lin, J.-H. and Ma, Y.-R., One-dimensionalmetal-oxide nanostructures: recent developments in synthesis, characterization, and applications, Adv. Funct. Mater. 22 (2012) 3326-3370.
2. Cozzoli, P. D., Pellegrino, T. and Manna, L., Synthesis, properties and perspectives of hybrid nanocrystal structures, Chem. Soc. Rev., 35, (2006) 1195-1208.
3. Zeng, H. and Sun, S., Syntheses, properties, and potential applications of multicomponent magnetic nanoparticles, Adv. Funct. Mater., 18, (2008) 391400.
4. Férey, G., Some suggested perspectives for multifunctional hybrid porous solids. Dalton Trans., 23, (2009) 4400-4415.
5. M. Suzuki, M., Kudo, K., Kojima, K., Yasue, T., Akutsu, A., Dino, W. A., Kasai, H., Bauer, E., and Koshikawa, T.,. Magnetic domain patterns on strong perpendicular magnetization of Co/Ni multilayers as spintronics materials: I. Dynamic observations, J. Phys. Condens. Matter., 25 (2013) 406001.
6. Johll, H., Lee, M. D., Ng, S. P., Kang, H. C. and Tok, E. S., Influence of inter configurational electronic states on Fe, Co, Ni-Silicene materials selection for spintronics, Sci. Rep. 4, (2014) 7594.
7. Shia, Y. and Zhang, B., Recent advances in transition metal phosphide nanomaterials: Synthesis and applications in hydrogen evolution reaction. Chem. Soc. Rev. , 45, (2016) 1529-1541.
8. Nardi, K. L., Yang, N., Dickens, C. F., Strickler, A. L. and Bent, S. F., Creating highly active atomic layer deposited NiO electrocatalysts for the oxygen evolution reaction, Adv. Energy Mater., 5, (2015) 1500412.

9. Deraz, N. M, Formation and magnetic properties of metallic nickel nano-particles, Int. J. Electrochem. Sci., 7, (2012) 4608 - 4616
10. Estrader, M., L´opez-Ortega, A., Estrad´e, S., Golozovsky, I. V., Salazar-Alvarez, G., Vazilakaki, M.,Trohidou, K. N., Varela, M., Stanley, D. C., Sinko, M., Pechan, M. J., Keavney, D. J., Peir´o, F., Suri˜nach, S., Bar´o, M. D. and Nogu´es, J., Robust antiferromagnetic coupling in hard-soft bi-magnetic core/shell nanoparticles, Nat. Commun., 4, (2013) 1-8.
11. Yao, X.-J. , He, X.-M., Song, X.-Y., Ding, Q., Li, ., Z.-W., Zhong, W., Au, C.-T. and Du, Y.-W., Enhanced exchange bias and coercivity arising from heterojunctions in Ni–NiO nanocomposites, Phys.Chem. Chem. Phys., 16 (2014) 6925-6930.
12. Nogués, J.; Langlais, V.; Sort, J.; Doppiu, S.; Suriñach, S.; Baró, M. D., Magnetic properties of Ni-NiO (ferromagnetic-antiferromagnetic) nanocomposites obtained from a partial mechanochemical reduction of NiO, J. Nanosci. Nanotechnol., 8, (2008) 2923-2928.
13. Yan, X., Tian, L., and Chen, X., Crystalline/amorphous Ni/NiO core/shell nanosheets as highly active electrocatalysts for hydrogen evolution reaction, J. Power Sources, 300 (2015) 336-343.
14. Song, S., Yao, S., Cao, J., Di, L., Wu, G., Guan, N. And Li, L., Heterostructured Ni/NiO composite as a robust catalyst for the hydrogenation of levulinic acid to γ-valerolactone, Appl. Catal. B. 217, (2017) 115-124.
15. Mallick1, P. and Mishra, N. C., Evolution of Structure, Microstructure, Electrical and Magnetic Properties of Nickel Oxide (NiO) with Transition Metal ion Doping, American Journal of Materials Science, 2 (2012) 66-71.
16. Sun, X., Si, W., Liu, X., Deng, J., Xi, L., Liu, L., Yan, C. and Schmidt, O.G., Multifunctional Ni/NiO hybrid nanomembranes as anode materials for high-rate Li-ion batteries, Nano Energy, 9 (2014) 168-175.
17. Yan, X., Tong, X., Wang, J., Gong, C., Zhang, M. and Liang, L., Construction of three-dimensional porous nano-Ni/NiO nanoflake composite film for electrochemical energy storage, Mater. Lett. 106, (2013) 250-253.
18. Mandal, S., Menona, S. R. K., Mahatha, S. K., Banerjee, S., Finite size versus surface effects on magnetic properties of antiferromagnetic particles, 99 (2011) 232507.
19. Liu, T., Pang, Y., Xie, X., Qi, W., Wu, Y., Kobayashi, S., Zheng, J. and Li, X. Synthesis of microporous Ni/NiO nanoparticles with enhanced microwave absorption properties, J. All. Compd., 667 (2016) 287-286.
20. Xiang, W., Liu, Y., Yao, J. and Sun, R., Influence of annealing temperature on the microstructure and magnetic properties of Ni/NiO core-shell nanowires, Phys. E., 97, (2018) 363-367.
21. Chaghouri, H.A., Tuna, F. Santhosh, P. N.,Thomas, P. J., Tiny Ni–NiO nanocrystals with exchange bias induced room temperature ferromagnetism, Solid State Commun., 230 (2016) 11-15.
22. Obradović, N., Fahrenholtz, W. G., Filipović, S., Corlett, C., Đorđević, P., Rogan, J., Vulić, P. J., Buljak, V., Pavlović, V., Characterization of $MgAl_2O_4$ Sintered Ceramics, Science of Sintering, 51 (2019) 363-376.
23. Filipović, S., Anđelković, Lj., Jeremić, D., Vulić, P., Nikolić, A. S., Marković, S., Paunović, V., Lević, S., Pavlović, V. B., Structure and Properties of Nanocrystalline

Tetragonal $BaTiO_3$ Prepared by Combustion Solid State Synthesis, Science of Sintering, 52 (2020) 1-12.
24. N. M. Deraz, Facile and eco-friendly route for green synthesis of magnesium ferrite nano particles, Science of Sintering, 52 (2020) 53-65.
25. Deraz, N. M., Selim, M. M. and Ramadan, M., Processing and properties of nanocrystalline Ni and NiO catalysts, Materials Chemistry and Physics, 113 (2009) 269-275.
26. Deraz, N. M., Magnetic behavior and physicochemical properties of Ni/NiO nanoparticles, Current Applied Physics, 12 (2012) 928- 934.
27. Madhumitha, G., Roopan, S. M., Devastated crops: multifunctional efficacy for the production of nanoparticles, J. Nanomater. (2013) 1-12. Article ID 951858, doi: 10.1155/2013/951858.
28. Kuppusamy P., Yusoff, M. M., Maniam, G. P., Govinda N., Biosynthesis of metallic nanoparticles using plant derivatives and their new avenues in pharmacological applications – an updated report. Saudi Pharm. J., 24, (2016) 473-484.
29. Prasad, Ch., Gangadhara, S. and Venkateswarlu, P., Bio-inspired green synthesis of $Fe_3O_4$ magnetic nanoparticles using watermelon rinds and their catalytic activity, Appl Nanosci., 6 (2016) 797-802.
30. Cullity, B. D., Elements of X-ray Diffraction, Addison-Wesly Publishing Co. Inc., Ch. 14 (1976).
31. Adelere, I. A., Lateef, A. A., Novel approach to the green synthesis of metallic nanoparticles: the use of agro-wastes, enzymes and pigments, Nanotechnol. Rev., 5, (2016) 567-587.
32. Jeon, Y. T., Moon, J. Y. , Lee, G. H., Park, J., Chang, Y., Comparison of the magnetic properties of metastable hexagonal close-packed Ni nanoparticles with those of the stable face centered cubic Ni nanoparticles, Journal of Physical Chemistry B, 110, (2006) 1187-1191.
33. Rodr´ıguez-Gonz´alez, V., Marceau, E., Beaunier, P., Che, M., and Train, C., Stabilization of hexagonal close-packed metallic nickel for alumina-supported systems prepared from Ni(II) glycinate, Journal of Solid State Chemistry, 180, (2007) 22-30,
34. Lee, H., Hong, M., Bae, S., Lee, H., Park, E., Kim, K., A novel approach to preparing nano-size $Co_3O_4$-coated Ni powder by the Pechini method for MCFC cathodes, Journal of Materials Chemistry, 13, (2003) 2626-2632.
35. Kakihana, M.,"'Sol-Gel' preparation of high temperature superconducting oxides," Journal of Sol-Gel Science and Technology, 6 (1996) 7-55.
36. Li, L., Chen, L., Qihe, R. and G. Li, Magnetic crossover of NiO nanocrystals at room temperature, Appl. Phys. Lett. 89, (2006) 134102.
37. Tsunekawa, S., Ishikawa, K., Li, Z. –Q., Kawazoe, Y., A. Kasuya, Origin of anomalous lattice expansion in oxide nanoparticles, Phys. Rev. Lett. 85 (2000) 3440.
38. Ayyub, P., Palkar, V. R., Chattopadhyay, S., M. Multani, Effect of crystal size reduction on lattice symmetry and cooperative properties, Phys. Rev. B, 51 (1995) 6135.
39. Rasband,W. S. ImageJ; U.S. National Institutes of Health: Bethesda, MD, USA, 1997.
40. Li, Y., Cai, M., Rogers, J., Xu, Y. and Shen, W.,"Glycerol mediated synthesis of Ni and Ni/NiO core-shell nanoparticles," Materials Letters, 60 (2006) 750-753.

41. Roy, A., Srinivas, V., Ram, S., De Toro, J. A., Mizutani, U., Structure and magnetic properties of oxygen-stabilized tetragonal Ni nanoparticles prepared by borohydride reduction method," Physical Review, B, 71 (2005) 184443-184410.
42. Lesnikovich, A. I., Sviridov, V. V., Printsev, G. V., Ivashkevich, O. A., Gaponik, P. N., A new type of self-organization in combustion, Nature, 323 (1986) 706.
43. Duan, W. J., Lu, S. H., Wu, Z. L., Wang, Y. S., Size Effects on Properties of NiO Nanoparticles Grown in Alkalisalts, J. Phys. Chem. C, 116 (2012) 26043.
44. Kakazey, M., Vlasova, M., Vorobiev, Y., Leon, I., Gonezalez, M. C., E. A. C. Urbiola, Processes of microstructural evolution during high-energy mechanical treatment of ZnO and black NiO powder mixture, Physica B, 453 (2014) 116.
45. A. C. Gandhi, C-Y Huang, C. C. Yang, T. S. Chan, C. L. Cheng, Y. R. Ma, S. Y. Wu, Nanos. Res. Lett. 6, 485 (2011).
46. Nogues, J., Schuller, I. K., Exchange bias, J. Magn. Magn. Mater., 192 (1999) 203.
47. Pillai, V., Shah, D. O., Synthesis of high-coercivity cobalt ferrite particles using water-in-oil microemulsions, J. Magn. Magn. Mater., 163 (1996) 243.

***Сажетак:*** *Ова студија је први покушај да се добије велика количина енергетски-ефикасном производњом наномагнетних Ni/NiO композита методом самосагоревања лишћа или екстракта из биљке corchorus olitorius. Синтетисани продукти могу бити карактерисани методама XRD, SEM, TEM и EDX. Резултати показују да је синтетисани материјал састављен из лепо искристалисаних фаза Ni и NiO. Кристалиничност Ni и NiO је побољшана порастом количине corchorus olitorius. Третман corchorus olitorius резултује повећањем величине кристалита и параметара решетке. SEM анализа потврђује формирање крхке, пахуљасте и сунђерасте мреже. Просечна величина зрна тако припремљених честица била је 45 nm и у сагласности са величином кросталита израчунатој из XRD анализе. Варирањем природе и садржаја биљке corchorus olitorius добијене су модификације у магнетним својствима, тачније Ms, Mr, Mr/Ms, Hc и Ka, добијеног Ni/NiO нанокомпозита услед структурне, морфолошке и микроструктурне промене. Сатурација магнетизације (Ms) узорка са лишћем биљке corchorus olitorius је 0.2383 emu/g док је Ms са екстрактом биљке corchorus olitorius износила 6.977 emu/g. Ово је дискутовано са аспекта коначне величине зрна и ефеката површине и интерфејса. Дакле, развили смо нови приступ синтезе сагоревањем лишћа биљке corchorus olitorius за директно добијање различитих нанокомпозита.*

***Кључне речи****: XRD, SEM, SBET, лишће corchorus olitorius, магнетна својства.*